Analysis and Suppression of Electromagnetic Ripple Torque of Surface-Mounted Permanent Magnet Synchronous Motor with Similar Number of Poles and Slots

Xiangdong Liu
School of Automation
Beijing Institute of Technology
Beijing, China
xdliu@bit.edu.cn

Yuan He
School of Automation
Beijing Institute of Technology
Beijing, China
18810964862@163.com

Quansong Mou
School of Automation
Beijing Institute of Technology
Beijing, China
18810933531@163.com

Jing Zhao*
School of Automation
Beijing Institute of Technology
Beijing, China
zhaojing_bit@.com

***Abstract*—In order to improve the positioning accuracy and stability of the servo system, the torque ripple of permanent magnet synchronous motor (PMSM) is analyzed. As the cogging torque and the reluctance torque of surface-mounted PMSM with similar number of poles and slots are small, the electromagnetic (EM) ripple torque caused by the interaction effect between back electromagnetic force (EMF) harmonics and armature current harmonics is the main component of the torque fluctuation. Firstly, the generation cause and the characteristics of EM ripple torque are analyzed and the 6th, 12th, 18th harmonics are the main components of the EM ripple torque. Then the rotor step skewing method and harmonic current compensation method are investigated and analyzed to reduce the EM ripple torque. Finally, the effectiveness of the two optimization methods are validated by finite element method (FEM) and prototype experiments.**

Keywords—Surface-mounted PMSM; electromagnetic ripple torque; rotor step skewing; harmonic current compensation.

I. INTRODUCTION

Because of its characteristics of high torque density, rapid dynamic response and high positioning accuracy, the permanent magnet synchronous motor (PMSM) is more and more used in high precision servo system [1-4]. In order to improve the accuracy of the servo system, the torque ripple of motor is needed to be eliminated. For, PMSM, the torque ripple is mainly divided into three kinds: 1) the cogging torque caused by the interaction between stator slots and permanent magnets (PMs); 2) the reluctance torque caused by saliency effects; 3) the electromagnetic ripple torque caused by the harmonics of back EMF and armature current [5-6]. All of the above ripple torque may lead to noise, vibration and control difficulties of PMSM and limit its applications in the high precision servo system.

For SPMSM, the reluctance torque generated by the asymmetrical magnetic field is generally negligible as the inductances L_d and L_q are basically equal [7-8]. Therefore, the main components which affects the torque fluctuation of PMSM are the cogging torque and EM ripple torque. To reduce them, many researches are studied including the structure optimization method and control compensation method [9]. The cogging torque can be reduced much by fractional slot winding [10-11], permanent magnet shape optimization [12-15], slot opening width adjustment [16] and harmonic current injection method [16-18]. However, under the load condition, the EM ripple torque caused by distortion of back EMF and input current becomes the main components of torque fluctuation with the increase of winding current and armature reaction. [19-20] analyze the generation reason of EM ripple torque without considering the phase of harmonic back EMF and harmonic current. In order to suppress the ripple torque, [20] reduces the ripple torque by optimizing the pole arc coefficient. [21] adopts the iterative learning control strategy. [22] develops a surface-mounted magnetic pole structure composed of magnetic conductive metals and permanent magnets to improve the waveform of air gap magnetic field and the sinusoidal of back EMF under no-load condition to reduce the ripple torque.

Because the SPMSM studied in this paper has adopted the near pole slot structure and optimized the eccentricity of the permanent magnet, the cogging torque is small enough to be ignored. So this paper focuses on the electrical ripple torque analysis and reduction under load condition with harmonics of back EMF and input current considered. To suppress the electrical ripple torque, the rotor step skewing method with different steps and harmonic current compensation method with different frequency are analyzed. Finally, the simulation and experiment are implemented to verify the effectiveness of the two different proposed methods

II. RIPPLE TORQUE ANALYSIS

For a PMSM driven by sine wave, the back EMF and current of armature winding should be sine. However, in actual applications, the waveform of air gap magnetic field is difficult to be ideal sine. Under load condition, the distortion of back EMF waveform increases because of the armature reaction. Although the current modulated by Space Vector Algorithm (SVPWM) is almost a sine wave, it still contains high order harmonics which leads to EM ripple torque.

To analyze the EM ripple torque caused by high harmonics in back EMF and winding current, the assumptions are made as:

978-1-7281-3398-0/19/$31.00 ©2019 IEEE

978-1-7281-3398-0/19/$31.00 ©2019 IEEE

- Three phase windings are symmetrical and Y-connected. The stator current doesn't contain 3rd and multiple of 3rd harmonics.
- The core hysteresis loss and eddy current loss are ignored.
- The core material isn't saturated and the armature reaction is ignored.

At this time, the input electromagnetic power is

$$P_{m1} = \sum ei = e_A i_A + e_B i_B + e_C i_C \tag{1}$$

where e_A, e_B and e_C are the back EMF of three phase windings; i_A, i_B and i_C are the current of three phase windings. The winding current and back EMF in phase A are shown as (2) and (3).

$$\begin{aligned} i_A = {} & \sqrt{2} I_1 \cos wt + \sqrt{2} I_5 \cos(5wt + \phi_5) + \\ & \sqrt{2} I_7 \cos(7wt + \phi_7) \end{aligned} \tag{2}$$

$$\begin{aligned} e_A = {} & \sqrt{2} E_1 \cos(wt + \varphi_1) + \\ & \sqrt{2} E_3 \cos(3wt + \varphi_3) + \\ & \sqrt{2} E_5 \cos(5wt + \varphi_5) \end{aligned} \tag{3}$$

where ϕ_5 and ϕ_7 are the initial phase angle of the harmonic current; φ_1, φ_3 and φ_5 are the initial phase angle of the harmonic back EMF; w is the fundamental frequency. When the motor running, the output EM power is calculated as:

$$P_{m1} = P_{m2} \tag{4}$$

where T_{em} is the EM torque; Ω is the rotation velocity of machine.

When the three-phase symmetrical AC motor is in operation state, the air gap magnetic field is a rotation magnetic field with constant amplitude. The total energy storage doesn't change during steady operation stage. Without considering the iron loss, the input electromagnetic power is equal to the output electromagnetic power as:

$$P_{m1} = P_{m2} \tag{5}$$

The EM torque of a SPMSM considering back EMF harmonics is deduced as:

$$\begin{aligned} T_{em} = {} & \frac{3}{\Omega} \{ E_1 I_1 \cos\varphi_1 + E_5 I_5 \cos(\varphi_5 - \phi_5) + \\ & E_7 I_7 \cos(\varphi_7 - \phi_7) + \cdots + E_1 I_5 \cos(6wt + \\ & \varphi_1 + \phi_5) + E_5 I_1 \cos(6wt + \varphi_5) + \\ & E_1 I_7 \cos(6wt - \varphi_1 + \phi_7) + E_7 I_1 \cos(6wt + \\ & \varphi_7) + \cdots + E_5 I_7 \cos(12wt + \varphi_5 + \phi_7) + \\ & E_7 I_5 \cos(12wt + \varphi_7 + \phi_5) \cdots \} \end{aligned} \tag{6}$$

It is found that the constant torque is generated when the frequency of back EMF and phase current are equal. The 6*k*th harmonic torque is produced when the sum or difference of the frequency of back EMF and current is 6*k*. For example, the 6th harmonic torque is produced when the fundamental back EMF interacts with the 5th harmonic current or the 7th harmonic current. In addition, the 3rd harmonic of back EMF neither produces constant torque nor produces EM ripple torque.

For space vector pulse width modulation (SVPWM), the current harmonics during steady-state operation are small and the current can be assumed as ideal sine wave. The equation (6) can be simplified to:

$$\begin{aligned} T_{em} = {} & \frac{3}{\Omega} \{ E_1 I_1 \cos\varphi_1 + E_5 I_1 \cos(6wt + \\ & \varphi_5) + E_7 I_1 \cos(6wt + \varphi_7) + \\ & E_{11} I_1 \cos(12wt + \varphi_{11}) \cdots \} \end{aligned} \tag{7}$$

From equation (7), it is found that the EM ripple torque is still consisted of 6th, 12th, 24th harmonics under ideal current conditions. At this time, he EM ripple torque is calculated as:

$$\begin{aligned} T_r = {} & T_6 \cos(6wt + \gamma_6) + T_{12} \cos(12wt + \gamma_{12}) + \cdots \\ = {} & \sum_{k=1,2,\cdots}^{\infty} T_{6k} \cos(6kwt + \gamma_{6k}) \end{aligned} \tag{8}$$

where γ_6, γ_{12} are the initial angles of the EM ripple torque.

III. Optimization Measure

Based on the above analysis, the main components of electromagnetic ripple torque are 6kth harmonics. To reduce them, both structure optimization method and control compensation strategy are studied in this section, including the rotor step skewing method and harmonic current compensation strategy.

A. Rotor step skewing method

The EM ripple torque is periodic and its period is fixed. The angle of the skewing step can be determined by the magnitude of the EM ripple torque. In practical application, the rotor step skewing is generally used to approximate the skewed pole to simplify the processing. This paper mainly analyzes the torque fluctuation with different step number Np and skewed angle β. The diagram is shown as Fig. 1.

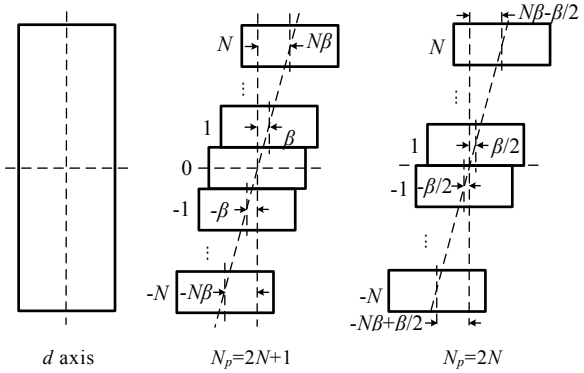

Fig. 1. The step skewing shceme of permanent magnet

The EM torque ripple after rotor step skewing reduction is deduced, as:

When N_p=2N+1

$$T_{rs}=\sum_{n=-N}^{-1}\sum_{k=1,2,\cdots}^{\infty}\frac{T_{6k}}{2N+1}\cos\left[6k\left(wt+np\beta\right)+\gamma_{6k}\right]+\sum_{n=1}^{N}\sum_{k=1,2,\cdots}^{\infty}\frac{T_{6k}}{2N+1}\cos\left[6k(wt+0\cdot\beta)+\gamma_{6k}\right]+\sum_{n=1}^{N}\sum_{k=1,2,\cdots}^{\infty}\frac{T_{6k}}{2N+1}\cos\left[6k\left(wt+np\beta\right)+\gamma_{6k}\right] \quad (9)$$

When N_p=2N

$$T_{rs}=\sum_{n=-N}^{-1}\sum_{k=1,2,\cdots}^{\infty}\frac{T_{6k}}{2N}\cos\left[6k\left(wt+p\frac{2n+1}{2}\beta\right)+\gamma_{6k}\right]+\sum_{n=1}^{N}\sum_{k=1,2,\cdots}^{\infty}\frac{T_{6k}}{2N}\cos\left[6k\left(wt+p\frac{2n-1}{2}\beta\right)+\gamma_{6k}\right] \quad (10)$$

Equations (9) and (10) are furthermore simplified as:

$$T_{rs}=\sum_{k=1,2,\cdots}^{\infty}\frac{T_{6k}}{N_p}\frac{\sin 3kpN_p\beta}{\sin 3kp\beta}\cos\left(6k\omega t+\gamma_{6k}\right) \quad (11)$$

where, p is the pole pairs. γ_{6k} is the initial phase of the electromagnetic torque.

It is found from (11) that if β satisfy

$$\beta=\frac{m\pi}{3pN_p}\quad m=1,2\cdots \quad (12)$$

the 6kth harmonics of the EM ripple torque will be reduced except for the 6kN_pth harmonic. With the increase of offset angle, the average EM torque decreases, so m is chosen as 1. At this time, the coefficient of the 6kN_pth harmonic is:

$$\frac{T_{6kN_p}}{N_p}\frac{\sin 3(kN_p)pN_p\beta}{\sin 3(kN_p)p\beta}=\frac{T_{6kN_p}}{N_p}\frac{N_p}{\cos(kN_p)p\beta}=(-1)^{mk}T_{6kN_p} \quad (13)$$

Equation (11) is simplified as:

$$T_{rs}=\sum_{k=1,2,\cdots}^{\infty}(-1)^{mk}T_{6kN_p}\cos\left[6kN_p\omega t+\gamma_{6kN_p}\right] \quad (14)$$

It is found that when N_p=2, the EM ripple torque only remains 12th harmonic and its multiple order harmonics. Besides, the amplitude of the residual ripple torque is constant, and its phase is related to m and harmonic order k. All the theoretical analyzed above are obtained on the assumptions that the core isn't saturated and there is no armature reaction. If the armature reaction is considered, the EM ripple torque becomes very complicated and difficult, and generally calculated by FEM.

B. Harmonic current compensation

The components of EM ripple torque are mainly 6th and multiple 6th harmonics. The fluctuation magnitude of harmonics decreases when its order increases. It can be seen from equation (6), that the 6th, 12th harmonic torque is generated when the fundamental back EMF reacts with harmonic current. Therefore, the EM ripple torque can be suppressed by harmonic current injection method.

For the SPMSM studied in this paper, the constant torque is produced when there is no transmission between the axis of stator magnetic potential and the axis of air gap synthetic magnetic field. Besides, for PMSM with three phase symmetrical windings, the magnitude of EM torque is concerned about the rotation magnetic fields produced by three phase winding and rotor magnetic pole. The EM torque can be calculated by magnetic co-energy based on the above analysis [23], as shown in (15):

$$T_{em}=-p\frac{\mu_0 l\pi D}{2g}F_1F_2\sin\delta_{12} \quad (15)$$

$$\delta_{12}=w_st-w_rt+\theta_0 \quad (16)$$

where l is the axil length of the motor; D represents the diameter of the armature; g is the length of the air gap; F_1 and F_2 represent the magnetomotive force of the stator and rotor, respectively; δ_{12} is the angle between them, expressed as (16). w_s and w_r are the rotation velocity of stator and rotor. θ_0 is the initial phase angle. The relationship between w_s and w_r can be divided into two kinds: one is w_s=w_r,, at this time, δ_{12} =θ_0, the EM torque is constant; the other is $w_s \neq w_r$, the EM torque is fluctuant and the fluctuation frequency is w_c= $|w_s - w_r|$.

To reduce the 6th harmonic torque of PMSM, the frequency of the expected ripple torque generated by injected harmonic current is w_c= 6w. As analyzed before, the 6th harmonic torque is produced when 5th or 7th harmonic compensation current is applied and reacts with the fundamental back EMF. When the compensation current is 5th harmonic, the phase sequence of it is A-C-B opposite to the fundamental current. When it is 7th harmonic, the phase sequence is A-B-C same with the fundamental current. High order harmonic torque produced during the cov mpensation process has little influence on torque waveform of PMSM as the amplitude of it is small. The initial phase angle of the harmonic and fundamental of back EMF are same under no load condition and it is different under load condition because of the armature reaction. Considering the two situations: one doesn't consider the armature reaction. At this time, the phase of harmonic compensation current is the same with that of fundamental current and deduced as equations (17) and (18). The other one considers armature reaction and the harmonic compensation current is calculated as (19) and (20).

$$i=\sqrt{2}I_1\cos\omega t+\sqrt{2}I_5\cos 5\omega t \quad (17)$$

or

$$i=\sqrt{2}I_1\cos wt+\sqrt{2}I_7\cos 7wt \quad (18)$$

$$i=\sqrt{2}I_1\cos wt+\sqrt{2}I_5\cos(5wt+\phi_5) \quad (19)$$

or

$$i=\sqrt{2}I_1\cos wt+\sqrt{2}I_7\cos(7wt+\phi_7) \quad (20)$$

IV. ANALYZED BY FEM

In this section, a 36-slot 34-pole SPMSM is utilized to validate the analysis before. The structure of the analyzed PMSM is shown as Fig. 2. To reduce the influence of the reluctance torque and the cogging torque, the polar arc

coefficient of the permanent magnet is 1.0 and the main parameters of paper is illustrated in TABLE □.

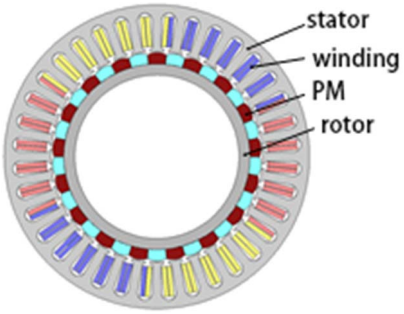

Fig. 2. The analysis model of PMSM

TABLE I. THE MAIN PARAMETERS OF PMSM

Parameters	value
Rated torque	3*Nm*
Outer diameter of the motor	110*mm*
Inner diameter of the motor	73*mm*
Number of slots	36
Number of poles	34
Pole arc coefficient	1.0
Offset of the permanent magnet	30*mm*

A. The electromagnetic ripple torque without suppression

The torque waveform of 36-slot 34-pole PMSM under rated load condition is calculated by FEM, and the results are shown as Fig. 3. It is found that the 6th harmonic is the main component of the torque ripple. The 2nd harmonic torque is mainly caused by the reluctance torque and the amplitude of it is small.

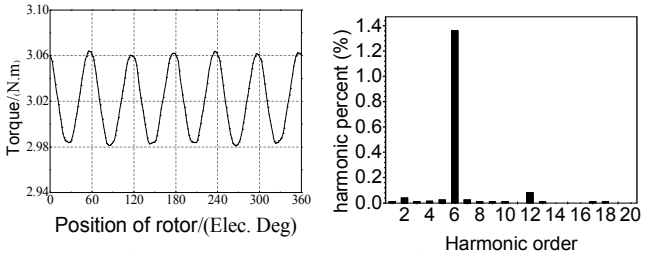

（a）torque waveform （b）harmonic analysis

Fig. 3. The torque waveform and spectrogram

B. Rotor step skewing method

For rotor step skewing method, the PMs are segmented and skewed with a certain offset along the axial direction of PMSM. The local magnetic field distortion occurs at the disconnections and the consistency of the magnetic field distribution is affected by the axial end effect. To consider the influences of them, the model of PMSM with rotor step skewing method applied can be established by 3D FEM at directions r, θ and z. However, such simulation is large hardware resources occupying, time consuming and seriously affected by mesh operation. Therefore, in practical engineering, the local field distortion and axil end effect are ignored and the step skewing method is qualitatively and quantitatively analyzed by 2D FEM. The offset of the PMs are calculated according to equation (12). The torque characteristics with different step number of PMs calculated by FEM are shown in TABLE Ⅰ and Fig. 4. T_{av} is the average value of torque. κ represents the torque fluctuation.

$$\kappa = \frac{T_{max} - T_{min}}{2T_{av}} \times 100\% \tag{21}$$

where T_{max} and T_{min} represent the maximum value and minimum value, respectively

TABLE II. THE AVERAGE TORQUE AND TORQUE RIPPLE WITH DIFFERENT STEP NUMBER

Serial number	Np=1		Np=2		Np=3		Np=4		Np=5		Np=6		Np=7	
	Tav	*κ(%)*	*Tav*	*κ(%)*	*Tav*	*κ(%)*	*Tav*	*κ(%)*	*Tav*	*κ(%)*	*Tav*	*κ(%)*	*Tav*	*κ(%)*
-3	-	-	-	-	-	-	-	-	-	-	0.46	0.98	0.39	0.95
-2	-	-	-	-	-	-	0.70	1.03	0.55	1.00	0.49	1.13	0.42	1.09
-1	-	-	1.47	1.13	0.95	1.05	0.75	1.29	0.59	1.18	0.50	1.30	0.43	1.24
0	3.02	1.37	-	-	1.01	1.37	-	-	0.60	1.37	-	-	0.43	1.37
1	-	-	1.45	1.65	0.93	1.77	0.75	1.49	0.59	1.60	0.50	1.45	0.43	1.51
2	-	-	-	-	-	-	0.69	1.78	0.55	1.78	0.48	1.65	0.41	1.70
3	-	-	-	-	-	-	-	-	-	-	0.46	1.77	0.38	1.78
sum	3.02	1.37	2.92	0.34	2.89	0.32	2.90	0.29	2.88	0.30	2.89	0.30	2.89	0.29

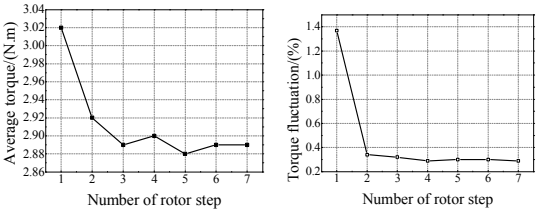

（a）average torque （b）torque fluctuation

Fig. 4. average torque and torque fluctuation with different step number

As shown in Fig. 4 and TABLE Ⅱ, when the rotor step skewing method is applied, the average torque decreases by 3.3% approximately without any influence of step number. Besides, the torque fluctuation decreases from 1.37% to 0.34% when $N_p = 2$. And when $N_p \geq 2$, the torque fluctuation are all around 0.3% without any influence of step number. To simply the processing, the step number N_p studied in this paper is chosen as 2.

The theoretic analysis before shows that the main component of ripple torque with step skewing method compensation is $6kN_p$th harmonic. However, the simulation results in TABLE Ⅱ and Fig.4 are different from it. For example, the left harmonic torque should be 12th calculated from the theoretical analysis when the step number of PMs is 2. But the main harmonics of ripple torque obtained by FEM are still 6th. The electrical angle difference of the two torque waveform is 180 degrees when the direction of the offset angle is opposite, as shown in Fig. 5. While the peak to peak value of them are different which affects the reduction effect of the 6th harmonics of EM ripple torque. The difference between them is mainly caused by the armature reaction and the saturation of stator core. To analyze it furthermore, assuming

that the offset direction of PMs is positive when it's the same with the rotation direction of PMSM and vice versa. The torque fluctuation with different offset angle are shown in Fig. 6. Since the harmonics of the EM ripple torque are 6th and multiple of 6th, the offset electrical angle varies within the range of -30 degrees to 30 degrees. As shown in Fig. 6, the torque fluctuation increases with the positive offset and it decreases when the offset is negative. When the skewed direction of PMs is positive, it is equivalent to the phase lag of the armature winding current and the d-axis current is magnetically enhanced leading to the increase of the saturation, average torque and torque fluctuation of PMSM. When the skewed direction is negative, the d-axis current is phase leading and its demagnetization effect leads to the decrease of the average torque and torque fluctuation.

Because of the armature reaction and the nonlinearity of core material, the saturation and torque fluctuation are different with opposite skewed direction of PMs. Therefore, the electromagnetic ripple torque cannot be completely reduced.

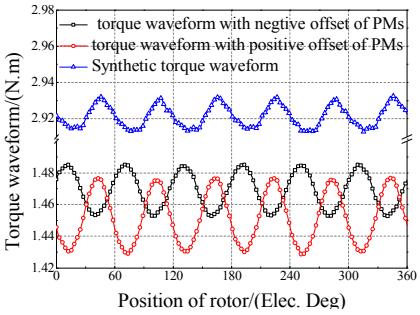

Fig. 5. The torque waveform with 2-step rotor

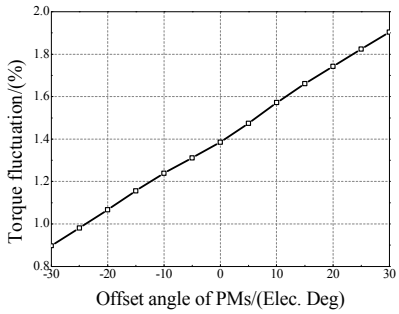

Fig. 6. The torque ripple with different PM shifting angle

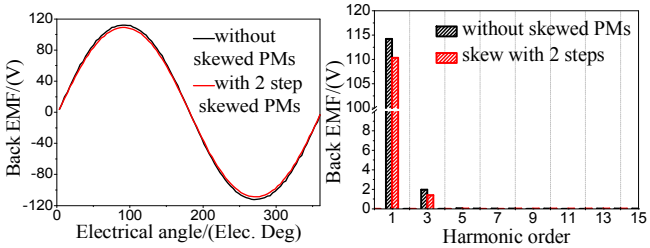

Fig. 7. Back EMF and its harmonic analysis for PMSM with 2-step rotor

Based on the above analysis, to reduce the torque fluctuation and simplify processing, the step number of rotor is chosen 2, and the shift angle of the PMs is -30 degrees. At this time, the back EMF and its harmonic analysis for PMSM are shown in Fig. 5. The fundamental amplitude of the back EMF decreases from 114.2V to 110.4V by 3.3% with the rotor step skewing method applied. And the EM torque decrease by 3.3% concluded from equation (7) which agrees with the conclusion in Fig. 4. Besides, the 5th and 7th harmonics of back EMF are reduced much, especially the 5th harmonic decreases by 76.8%.

C. *Harmonic current compensation*

From the Fourier decomposition obtained before, the phase angle of the 6th harmonic torque is $\gamma 6=25°$, so the phase angles of the 5th and 7th harmonic compensation currents are , calculated by equations (19) and (20). The torque characteristics with different harmonic current compensation are calculated by FEM and the results are shown in Fig. 8. It is found that both 5th and 7th harmonic compensation currents can suppress the torque fluctuation. And the compensation effect is better when the initial phase of compensation current is considered. Besides, the average torque with 5th harmonic current compensation is less than that with 7th harmonic, because of its phase sequence. The phase sequence of the 5th harmonic compensation current is opposite to fundamental current, thus the torque produced by it is also opposite to the torque produced by fundamental current, leading to the decrease of average torque. While 7th harmonic current has the same phase sequence with fundamental current and the average torque increases.

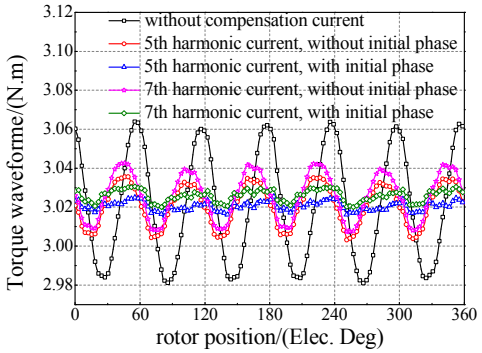

Fig. 8. The torque waveform with current compensation

V. VALIDATED BY EXPERIMENT

To verify the effectiveness of the rotor step skewing method, the rotor with and without rotor skewed are manufactured, as Fig. 9 shown. The theoretical analysis is verified by testing the back EMF of armature windings indirectly. The tested back EMF waveform and its harmonic spectrum under no-load condition are shown in Fig. 10.

Fig. 9. The prototype and the experiment system

As shown in Fig. 10, the fundamental amplitude of the back EMF decreases from 110.4V to 106.8V by 3.2% after the rotor step skewing method is applied. The back EMF calculated by FEM in Fig.7 decreases by 3.3%. They are in great agreement. Assuming that the armature current is ideal sine wave and it has the same phase with the fundamental back

EMF, the experimental test of EM torque decrease by 3.2% concluded from equation (7). Compared with the simulation results in Table 2 in which the average torque decreases from 3.02N to 2.92N by 3.3% calculated by FEM. The measured values are in good agreement with the simulation results. Besides, the 5th and 7th harmonics of back EMF are reduced much, especially the 5th harmonic decreases by 65.6%. As analyzed before, the 3rd harmonic of back EMF do not generate EM harmonic torque, so the rotor step skewing method can reduce the electromagnetic ripple torque effectively.

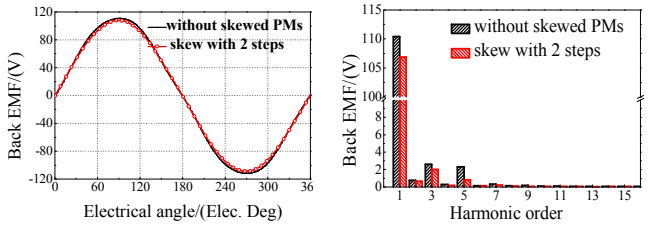

（a）Back EMF by experiment （b）Harmonic spectrum

Fig. 10. Experimental results of Back EMF and harmonic analysis

VI. Conclusion

The EM ripple torque of SPMSM with similar number of poles and slots is theoretically analyzed in this paper. It is concluded that the main components of the EM ripple torque are 6th and multiple of 6th harmonics hen the harmonics exist in both back EMF and armature winding current. Then, rotor step skewing method and harmonic current compensation method are analyzed to suppress the EM ripple torque. Corresponding simulations are implemented by FEM to verify the theoretic analysis. The simulation consequent of the rotor step skewing method is not as effective as theoretic analysis because of the armature reaction and core saturation. In addition, with rotor step skewing, the average torque and torque fluctuation both decrease with little influence of step number. Compared with the rotor step skewing method, the harmonic current injection method has smaller torque fluctuation and does not reduce the average torque. But the control strategy will be slightly complicated.

Acknowledgment

This paper was supported in part by the National Natural Science Foundation of China under Projects 51677005, and the Intelligent Equipment and Technology of Automation Research and Development Platform under Grant 2016F2FC007.

References

[1] H Wang, Y Yu, D Xu. "The position servo system of PMSM". *Proceedings of the CSEE*, vol. 24, no. 7, pp. 151-155, 2004

[2] N. Bianchi, S. Bolognani and P. Frare, "Design criteria for high-efficiency SPM synchronous motors," in *IEEE Transactions on Energy Conversion*, vol. 21, no. 2, pp. 396-404, June 2006.

[3] H. Hu, J. Zhao, X. Liu, Z. Chen, Z. Gu and Y. Sui, "Research on the Torque Ripple and Scanning Range of an Arc-Structure PMSM Used for Scanning System," in *IEEE Transactions on Magnetics*, vol. 50, no. 11, pp. 1-4, Nov. 2014, Art no. 8105504.

[4] B. Li, J. Zhao, X. Liu, Y. Guo, H. Hu and J. Li, "Detent Force Reduction of an Arc-Linear Permanent-Magnet Synchronous Motor by Using Compensation Windings," *in IEEE Transactions on Industrial Electronics*, vol. 64, no. 4, pp. 3001-3011, April 2017.

[5] R. Islam, I. Husain, A. Fardoun and K. McLaughlin, "Permanent-Magnet Synchronous Motor Magnet Designs With Skewing for Torque Ripple and Cogging Torque Reduction," in *IEEE Transactions on Industry Applications*, vol. 45, no. 1, pp. 152-160, Jan.-feb. 2009.

[6] D. Ting, W. Ruiqing, Z. Jicheng and L. Kun, "Influence of auxiliary slot on electromagnetic vibration in PMSM with similar slot and pole number," *2017 20th International Conference on Electrical Machines and Systems (ICEMS)*, Sydney, NSW, 2017, pp. 1-5.

[7] W. Tong, R. Sun, C. Zhang, S. Wu and R. Tang, "Loss and Thermal Analysis of a High-Speed Surface-Mounted PMSM With Amorphous Metal Stator Core and Titanium Alloy Rotor Sleeve," in *IEEE Transactions on Magnetics*, vol. 55, no. 6, pp. 1-4, June 2019, Art no. 8102104.

[8] Y. Shi, J. Chai, X. Sun and S. Mu, "Detailed description and analysis of the cross-coupling magnetic saturation on permanent magnet synchronous motor," in *The Journal of Engineering*, vol. 2018, no. 17, pp. 1855-1859, 11 2018.

[9] M. Wang, L. Li and D. Pan, "Detent Force Compensation for PMLSM Systems Based on Structural Design and Control Method Combination," *in IEEE Transactions on Industrial Electronics*, vol. 62, no. 11, pp. 6845-6854, Nov. 2015.

[10] M. Farshadnia, R. Dutta, J. E. Fletcher, K. Ahsanullah, M. F. Rahman and H. C. Lovatt, "Analysis of MMF and back-EMF waveforms for fractional-slot concentrated-wound permanent magnet machines," *2014 International Conference on Electrical Machines (ICEM)*, Berlin, 2014, pp. 1976-1982.

[11] K. Ahsanullah, R. Dutta and M. F. Rahman, "Analysis of Low-Speed IPMMs With Distributed and Fractional Slot Concentrated Windings for Wind Energy Applications," in *IEEE Transactions on Magnetics*, vol. 53, no. 11, pp. 1-10, Nov. 2017, Art no. 3101710.

[12] F. Chai, P. Liang, Y. Pei and S. Cheng, "Magnet Shape Optimization of Surface-Mounted Permanent-Magnet Motors to Reduce Harmonic Iron Losses," in *IEEE Transactions on Magnetics*, vol. 52, no. 7, pp. 1-4, July 2016, Art no. 6301304.

[13] P. Zheng, J. Zhao, J. Han, J. Wang, Z. Yao and R. Liu, "Optimization of the Magnetic Pole Shape of a Permanent-Magnet Synchronous Motor," in *IEEE Transactions on Magnetics*, vol. 43, no. 6, pp. 2531-2533, June 2007.

[14] N. Chen, S. L. Ho and W. N. Fu, "Optimization of Permanent Magnet Surface Shapes of Electric Motors for Minimization of Cogging Torque Using FEM," in *IEEE Transactions on Magnetics*, vol. 46, no. 6, pp. 2478-2481, June 2010.

[15] H. Liu, I. Kim, Y. J. Oh, J. Lee and S. Go, "Design of Permanent Magnet-Assisted Synchronous Reluctance Motor for Maximized Back-EMF and Torque Ripple Reduction," in *IEEE Transactions on Magnetics*, vol. 53, no. 6, pp. 1-4, June 2017, Art no. 8202604.

[16] T. Liu, S. Huang, J. Gao and K. Lu, "Cogging Torque Reduction by Slot-Opening Shift for Permanent Magnet Machines," in *IEEE Transactions on Magnetics*, vol. 49, no. 7, pp. 4028-4031, July 2013.

[17] J. Lu, J. Yang and Y. Ma, "Research on harmonic compensation for flux and current of permanent magnet synchronous motor," *2015 IEEE International Conference on Advanced Intelligent Mechatronics (AIM)*, Busan, 2015, pp. 589-594.

[18] H. Jia, M. Cheng, W. Hua, W. Zhao and W. Li, "Torque Ripple Suppression in Flux-Switching PM Motor by Harmonic Current Injection Based on Voltage Space-Vector Modulation," in *IEEE Transactions on Magnetics*, vol. 46, no. 6, pp. 1527-1530, June 2010.

[19] S. Jang, H. Park, J. Choi, K. Ko and S. Lee, "Magnet Pole Shape Design of Permanent Magnet Machine for Minimization of Torque Ripple Based on Electromagnetic Field Theory," in *IEEE Transactions on Magnetics*, vol. 47, no. 10, pp. 3586-3589, Oct. 2011.

[20] W. Zhang, S. Huang, J. Gao, R. Li and L. Dai, "Electromagnetic Torque Analysis for All-Harmonic-Torque Permanent Magnet Synchronous Motor," in *IEEE Transactions on Magnetics*, vol. 54, no. 11, pp. 1-5, Nov. 2018, Art no. 8206405.

[21] S. Mandra, K. Galkowski, E. Rogers, A. Rauh and H. Aschemann, "Performance-Enhanced Robust Iterative Learning Control With Experimental Application to PMSM Position Tracking," in *IEEE Transactions on Control Systems Technology*, vol. 27, no. 4, pp. 1813-1819, July 2019.

[22] B Zhang, Y Jia, K Li, etc. "Study on magnetic pole structure of surface mounted PMSM, ". *Electric Machine and Control,* vol. 18, no. 5, pp. 43-48, 2014.

[23] Y Tang, Y Luo, Y Liang. Electrical Machinery. Beijing: Mechanical Industry Press, 2008